Energetics of the $Al^{27}(B^{11},p3n)Cl^{34m}$ Reaction from Recoil Studies*

MORTON KAPLAN† AND ALAN EWART
Department of Chemistry, Yale University, New Haven, Connecticut
(Received 28 March 1966)

We have studied, in detail, the $Al^{27}(B^{11},p3n)Cl^{34m}$ reaction at bombarding energies from 30 to 115 MeV. This paper presents measurements of cross sections, average recoil ranges, and angular distributions of the reaction product Cl^{34m}, the high-spin member of an isomeric pair. The excitation function behavior is unusual, exhibiting a relatively slow decrease in cross section at higher energies. The peak cross section is about 16 mb, and at 65 MeV above the excitation-function peak, the cross section is approximately 2% of its maximum value. Our recoil range results provide strong evidence that the reaction proceeds by compound-nucleus formation at all energies investigated. At the highest bombarding energy, approximately 66 MeV must be dissipated as particle kinetic energies and photons in the compound nucleus de-excitation. The analysis of our angular-distribution experiments indicates that most of this energy appears as kinetic energy of emitted particles. The total particle kinetic energy increases approximately linearly with available energy. Relatively little de-excitation energy is released in the form of gamma radiation, of the order of 7 MeV or less. The trend of total gamma-ray emission energy with increasing available energy is roughly constant, but seems to show a slight decrease. There is no direct evidence that the formation of Cl^{34m} involves preferential selection of compound nuclei with greater than average angular momentum. On the contrary, if the presence of gamma-ray competition with particle evaporation is taken as a criterion of high angular momentum, then our results may imply a strong discrimination against high-angular-momentum events. Our range-energy data for Cl^{34m} in Al are compared with the predictions of stopping theory. The high velocities encountered in our experiments provide a test of the theoretical formulation relating to electronic stopping. Although general agreement is good, there are systematic deviations which may indicate the approximate character of the theoretical assumptions.

I. INTRODUCTION

THE careful investigation of the recoil properties of residual nuclei from nuclear reactions may yield significant information on energy and momentum processes occurring in the reactions.[1] In particular, for compound-nucleus reactions the resultant linear momentum vector of the reaction product will be determined by the incident-beam momentum appropriately coupled to the recoil vectors arising from particle emission. If the momentum transfer in compound-nucleus formation is substantially greater than the momentum effects of subsequent de-excitation, then the average range of the recoiling reaction product (in some stopping medium) will be determined primarily by the initial impact. The distribution in ranges about the average value will result from the recoil velocity distribution due to particle evaporation, from straggling inherent in the stopping process, and from experimental effects. Thus, average range measurements are useful in determining whether a reaction involves compound-nucleus formation, but interpretation of range straggling data may be complex.

The angular distribution of the recoiling products, on the other hand, arises directly from the momentum effects in the compound-nucleus decay (since the initial impact involves a momentum component only along the beam direction). By carrying out appropriate experiments and analyses, angular-distribution data may be related to the energetics of the de-excitation processes.

In this paper we report results of cross section, average recoil range, and angular distribution measurements for the $Al^{27}(B^{11},p3n)Cl^{34m}$ reaction over a wide region of bombarding energy. The primary purpose of the work was to determine if the reaction proceeded by means of a compound-nucleus mechanism, and if so, to obtain an estimate of the distribution of de-excitation energy into particle emission and gamma-ray emission. Previous studies of products from heavy-ion induced compound-nucleus reactions have indicated significant differences in gamma-ray competition for Tb^{149g} compared to Dy products.[2,3] The observed effects may be correlated with the fact that Tb^{149g} is the low-spin member of an isomeric pair and hence may represent a nontypical sampling of the distribution of angular-momentum states in the excited compound nuclei. In particular, Tb^{149g} might be formed preferentially by decay of compound nuclei of lower than average angular momentum, whereas the Dy products would result from a (presumably) statistical distribution of spin states. In the present work, the reaction product Cl^{34m} is the high-spin member of an isomeric pair, and it was of considerable interest to investigate the role of gamma-ray competition for this case.

An additional result of the experiments to be described is a comparison of the measured average ranges for Cl^{34m} with the predictions of stopping theory. In the $Al^{27}(B^{11},p3n)Cl^{34m}$ reaction at the bombarding energies involved here (30–115 MeV), the product of a full-momentum-transfer process will have a forward recoil

* This work has been supported by the U. S. Atomic Energy Commission.
† Alfred P. Sloan Foundation Fellow.
[1] B. G. Harvey, Ann. Rev. Nucl. Sci. **10**, 235 (1960).
[2] G. N. Simonoff and J. M. Alexander, Phys. Rev. **133**, B104 (1964).
[3] J. M. Alexander, J. Gilat, and D. H. Sisson, Phys. Rev. **136**, B1289 (1964).

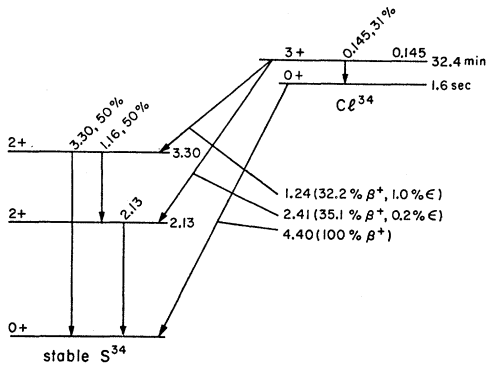

FIG. 1. Decay scheme of the Cl^{34} isomers.

velocity comparable to a fission fragment. At these rather high velocities, theory indicates that the dominant contribution to the stopping process arises from interactions with the electrons of the stopping medium, and we shall use our data to test the validity of the theoretical formulation in this relatively unexplored region.

II. EXPERIMENTAL PROCEDURES

In this section we shall describe the techniques used in our measurements, beginning with those features which are common to all of the work. Then will follow a discussion of the particular procedures which were involved in the different types of experiments.

In each experiment, an Al-foil target, mounted with an appropriate array of catcher foils, was irradiated with a beam of B^{11} ions from the Yale heavy-ion accelerator. After bombardment, the target and/or catchers were chemically processed,[4] and the resulting samples were assayed for Cl^{34m} β radioactivity using a series of end-window methane-flow proportional counters. The decay scheme[5] of Cl^{34m} is shown in Fig. 1. This species decays with a 32.4-min half-life to the ground state of Cl^{34} by isomeric transition and to states in S^{34} by positron emission. The ground state of Cl^{34} decays by positron emission to S^{34}. The half-life of the ground state of Cl^{34} is sufficiently short so that any Cl^{34g} formed directly in the irradiations has decayed, and the Cl^{34g} present in the samples is in radioactive equilibrium with the 32.4-min Cl^{34m} parent. All samples were counted through Al absorbers 432 mg/cm^2 thick to filter out low-energy radiations from impurities not completely removed in the chemical separation. Counting was continued for several half-lives, and the resulting decay curves showed no components other than 32.4-min Cl^{34m}. (Contamination from 38-min Cl^{38} is not possible in the $B^{11}+Al^{27}$ reaction.) The combination of chemical separation, counting through Al absorbers, and accumulation of decay curves permitted accurate determination of Cl^{34m} yields even in experiments where the counting rate per sample was quite low.[6]

In most experiments only relative counting rates of the samples were required. The eight counters used were independently adjusted with low-level discriminators to yield equal counting rates for a thick uranium standard. The intercalibration was checked by counting the same Cl^{34m} sample in several of the counters. Corrections for counter backgrounds and chemical yields of the samples[7] were applied to all of the data.

A. Recoil Ranges and Cross Sections

Our average range experiments were of the integral type,[1] consisting of measurements of the fraction of Cl^{34m} activity which recoils out of thick targets. The targets used were 1-in.-diam disks of commercial (99.5%-min purity) Al foil, and were individually weighed for accurate thickness determinations. The nominal thicknesses were 0.0005 in. at the higher bombarding energies and 0.00025 in. at the lower energies. These thicknesses corresponded roughly to twice the Cl^{34m} average ranges. The catcher foils were 1-in.-diam disks of nominal 0.001-in. Mylar, individually cleaned and weighed. Foil stacks consisting of several Al targets, Mylar catchers and Mylar blanks were irradiated in a water-cooled copper holder with B^{11} ions. The beam definition was determined by two $\frac{1}{4}$-in. collimators 20 in. apart located 10 in. from the target assembly. The desired incident-beam energies were obtained by inserting appropriate Al foils in the beam path and magnetically analyzing the degraded beam upstream from the collimator assembly. Beam energies in the targets were calculated from energy-loss measurements in aluminum[8] and Mylar.[9] Average beam currents were kept below 9 mμA to avoid burning the Mylar foils, and integrated beam fluxes were obtained with a magnetically shielded Faraday cup and Elcor electrometer.

The targets, catchers, and blanks were separated, after irradiation, chemically processed, and counted for

[4] The chemical procedure employed was as follows: The irradiated foils were dissolved in a suitable solvent (NaOH for Al foils, hot dimethyl formamide for Mylar foils, and HNO_3 for Cu foils), Cl^- carrier was added, and AgCl was precipitated, purified, and mounted for counting. Preliminary tests indicated this method of separation to be satisfactory, and no difficulty was encountered from higher oxidation states of Cl.

[5] *Nuclear Data Sheets*, compiled by K. Way *et al.* (National Academy of Sciences, National Research Council, U. S. Government Printing Office, Washington, D. C., 1960).

[6] In preliminary experiments, attempts were made to count the catcher foils without chemical separation of Cl. However, even with the use of Al absorbers, the decay curves obtained showed contamination which would significantly increase the uncertainty in the measurements, and thereafter chemical procedures were employed.

[7] Chemical yields were determined by volumetric titration of Cl with $Hg(NO_3)_2$ after the counting had been completed. The yields were consistently above 80% with only small variations from sample to sample.

[8] L. C. Northcliffe, Phys. Rev. **120**, 1744 (1960); Ann. Rev. Nucl. Sci. **13**, 67 (1963).

[9] P. E. Schambra, A. M. Rauth, and L. C. Northcliffe, Phys. Rev. **120**, 1758 (1960).

Cl^{34m} β radioactivity. Our procedure effectively eliminated all contaminating radioactivity from activation of the Mylar foils, and no blank corrections were necessary. The relative activities found in a target and corresponding catcher are related[1] to the average range of Cl^{34m} in the target material as follows:

$$R_0 = FW, \tag{1}$$

where R_0 is the average range (projected on the beam direction), F is the fraction of the total Cl^{34m} activity which recoils out of the target, and W is the target thickness.[10] Equation (1) assumes that the cross section for Cl^{34m} production is constant throughout a target thickness, which was not quite correct in some of our experiments, because of beam-energy loss in the target material. We have, therefore, used a modified relationship[11]

$$F = \frac{R_0}{W^2} \frac{2\sigma_x W + (\sigma_i - \sigma_x)R_0}{(\sigma_i + \sigma_x)} \tag{2}$$

to take cross-section changes into account. In Eq. (2), σ_i and σ_x are the cross sections corresponding to the incident and exit surfaces of the target, and the derivation[11] assumes a linear cross-section variation over the thickness of the target. The effect of Eq. (2), as compared to Eq. (1), is to decrease the average-range values at bombarding energies above the excitation-function maximum and to increase the average ranges at low energies. In the work reported here, the corrections amounted to about 4% at the higher energies, zero in the vicinity of the excitation-function peak, and 13% at the lowest energy, where beam degradation and changing cross section were most severe.

Cross-section data were obtained by summing the Cl^{34m} activity found in a target and corresponding catcher. The relative measurements were put on an absolute basis in a separate series of experiments in which Cl^{34m} samples with known disintegration rates were counted in the β-counter assemblies.[12]

The body of range and cross-section data was obtained in many independent runs, each of which overlapped in energy with another run. Each energy region was covered at least two times.

B. Angular Distributions

The experimental apparatus used for measuring angular distributions of Cl^{34m} recoils was very similar to that described previously.[2] A schematic diagram is shown in Fig. 2. Recoils escaping from a thin target traveled in vacuum and were caught on a catcher plate located at a known distance from the target. The catcher plate consisted of a 4-in.-diam stainless-steel cutter, with sharp circular blades accurately machined at $\frac{1}{8}$-in. radial intervals. Copper foil, 0.001 in. thick, was stretched over the cutting edges and after collection of recoils, the foil was cut into rings by means of an hydraulic press. Each ring corresponded to a well-defined angular interval.

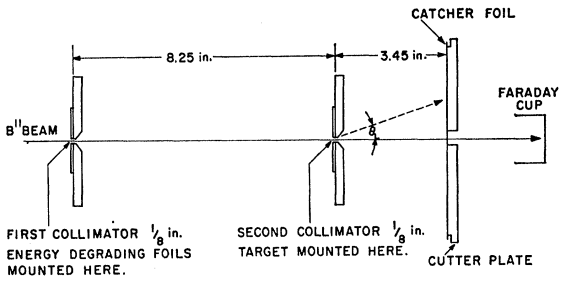

FIG. 2. Schematic diagram of the apparatus used in angular distribution experiments.

The cutter was calibrated in two independent ways. The first method consisted of cutting rings from several copper foils of known thickness, and determining the area of each ring from weight measurements. In the second method, the inner and outer diameters of each ring were directly measured with an image-shadow projection machine incorporating high magnification and a cathetometer. The separate calibrations all agreed to better than 1%. Under the conditions of our experiments, the target-catcher distance corresponded to an angular acceptance of roughly 2° per ring.

In our work, the Cl^{34m} recoils are kinematically restricted to a relatively narrow forward cone. Therefore, in order to obtain adequate angular resolution, it was important that the incident projectile beam be highly collimated. We have used two $\frac{1}{8}$-in.-diam collimators (see Fig. 2), resulting in a beam definition of approximately 1°. This arrangement was found to be an optimum balance between beam resolution and loss of intensity. For similar reasons of beam intensity, it was expedient to degrade the beam energy at the first collimator position. The influence of collimator size on the angular distributions will be discussed in Sec. III.

We have experimentally measured the effects of target thickness on the angular distributions by using targets of different thickness at several bombarding energies. This will also be discussed in detail in Sec. III.

After bombardment, the catcher foil was cut, each ring chemically processed, and the samples assayed for Cl^{34m}, as described above. As only relative activity measurements are required for eack angular distribution, absolute counter-efficiency corrections were not applied to the data.

[10] No Cl^{34m} radioactivity was ever detected in catchers placed upstream from an Al target. This implies that Cl^{34m} does not recoil into the backward direction, as required by the kinematics for a full momentum transfer process.

[11] J. P. Hazan and M. Blann, Phys. Rev. 137, 1202 (1965).

[12] Absolute disintegration rates were determined by intensity measurements of the 0.145-, 1.16-, and 2.13-MeV gamma rays (see Fig. 1) under conditions of known geometry and efficiency.

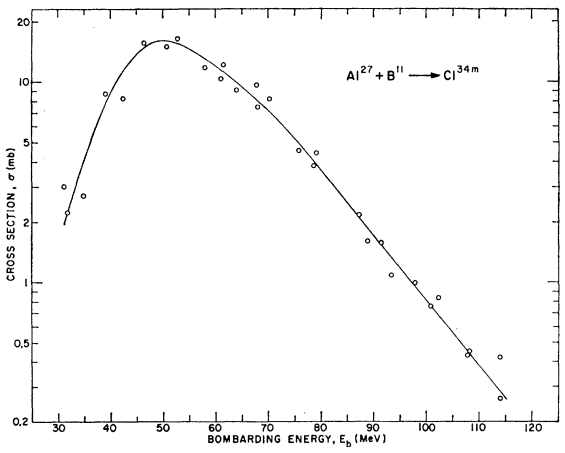

FIG. 3. Excitation function for the $Al^{27}(B^{11},p3n)Cl^{34m}$ reaction.

III. RESULTS AND DISCUSSION

A. Excitation Function and Recoil Ranges

We report in Table I our cross section and average recoil-range results for the $Al^{27}(B^{11},p3n)Cl^{34m}$ reaction. The first column gives the bombarding energy E_b computed at a point midway through the Al target of thickness W, listed in column 2. Typical energy losses as the beam traversed a target were 3–4 MeV, depending on target thickness and incident energy. Column 3 is the measured cross section. The recoil energies of Cl^{34m}, given in column 4, were computed assuming compound-nucleus formation in the $Al^{27}(B^{11},p3n)$ reaction. For a full-momentum-transfer process, with particle emission symmetric about 90° in the center-of-mass system, the product recoil energy is given by

$$E_R=\frac{A_bA_RE_b}{(A_b+A_T)^2}, \tag{3}$$

where E and A are energy and mass, respectively, with subscripts R for recoil product, b for beam projectile, and T for target nucleus. The fifth column in Table I is the product of the target thickness W by the fraction F of the total Cl^{34m} recoil activity which escapes from the target. The quantity FW would be equal to the average (projected) recoil range if the cross section for Cl^{34m} were constant through a target. Column 6 is the average recoil range R_0, projected along the beam direction, as given by Eq. (2). The differences between columns 5 and 6 reflect the applied corrections which take into account cross-section variations through the targets.

Figure 3 shows the excitation function for the $Al^{27}(B^{11},p3n)Cl^{34m}$ reaction.[13] The most prominent feature is the pronounced asymmetry resulting from the relatively slow decrease in cross section with increasing bombarding energy. At 65 MeV above the excitation-function peak, the cross section is approximately 2% of its maximum value. The full width at half-maximum is 29 MeV. The low-energy side of the excitation function is unaffected by a Coulomb-barrier cutoff, since the barrier is ~12 MeV whereas the reaction threshold is 21.8 MeV. As will be shown below, our range measurements provide very strong evidence that the reaction proceeds by a compound-nucleus mechanism over the full-energy region investigated, and consequently the high-energy "tail" of the excitation function cannot be attributed to a "change in mechanism" or "direct-interaction process." Measurement of the excitation function for the independent formation of 1.6-sec Cl^{34g} (the low-spin isomer) would be very illuminating.

It is interesting to note the magnitudes of the de-excitation energies which are associated with the energy range of Fig. 3. At the peak of the excitation function approximately 20 MeV must be dissipated as particle kinetic energies and photons. At a bombarding energy of 114 MeV, the corresponding value is 66 MeV. This

TABLE I. Cross section and average recoil-range results for the $Al^{27}(B^{11},p3n)Cl^{34m}$ reaction.

Bombarding energy, E_b (MeV)	Target thickness, W (mg/cm²)	Cross section, σ (mb)	Recoil energy, E_R (MeV)	FW (mg/cm²)	Average range, R_0 (mg/cm²)
114.0[a]	3.56	0.42	29.5[b]	2.35[c]	2.27[d]
114.1	3.44	0.26	29.5	2.47	2.40
108.3	3.48	0.45	28.0	2.06	1.96
107.8	3.42	0.43	27.9	2.22	2.14
102.3	3.55	0.83	26.5	2.24	2.17
100.9	3.42	0.75	26.1	2.09	2.05
98.0	3.48	0.98	25.4	2.33	2.23
93.4	3.44	1.08	24.2	1.92	1.83
91.5	3.54	1.57	23.7	1.95	1.88
88.8	3.56	1.59	23.0	1.80	1.73
87.4	3.26	2.16	22.6	2.01	1.94
79.1	3.26	4.39	20.5	1.78	1.71
78.6	3.56	3.79	20.4	1.79	1.73
75.8	3.46	4.52	19.6	1.77	1.70
70.2	3.30	8.19	18.2	1.63	1.56
68.0	3.44	7.45	17.6	1.74	1.66
67.8	3.46	9.64	17.5	1.72	1.65
64.0	3.56	9.04	16.6	1.32	1.25
61.5	3.24	12.1	15.9	1.47	1.40
61.0	3.44	10.3	15.8	1.58	1.52
57.9	3.44	11.8	15.0	1.44	1.38
52.7	3.44	16.4	13.6	1.30	1.26
50.7	3.26	14.9	13.1	1.21	1.21
46.4	3.59	15.4	12.0	1.20	1.28
42.5	3.46	8.22	11.0	0.94	1.14
39.1	1.66	8.74	10.1	1.10	1.17
34.9	1.67	2.70	9.0	0.915	1.03
32.0	1.67	2.23	8.3	0.943	1.07
31.3	3.44	3.01	...	...	...

[a] Refers to the center of the target. Typical beam-energy loss in the targets was 3–4 MeV.
[b] Calculated from Eq. (3).
[c] Fraction of the total activity escaping from a target, multiplied by the target thickness. This would give the average range if cross-section changes were negligible across the target.
[d] Computed from Eq. (2).

[13] We refer throughout this paper to the $Al^{27}(B^{11},p3n)$ reaction although our experiments would not distinguish this process from the $Al^{27}(B^{11},4n)Ar^{34}$ reaction, followed by beta decay. However, it is very unlikely that Cl^{34m}, with spin 3, would be populated by beta decay from the ground state of Ar^{34}.

large amount of energy, in a reaction in which only four nucleons are emitted, must lead to rather unusual energetics: either the particles have *very* high kinetic energies; or a large fraction of the energy is released as gamma rays; or some combination of these possibilities. We shall return to this question in Sec. IIIB, where the analysis of our angular-distribution experiments provides an answer.

The results of our integral range measurements are plotted in Fig. 4. The ordinate is the average range of Cl^{34m} in Al and the abscissa is energy. The points are the data from Table I. The solid line is an empirical fit to the data, given by

$$R_0=0.06E_R+0.52, \quad (4)$$

with E_R in MeV and R_0 in mg/cm². Equation (4) is not meant to imply any fundamental significance or uniqueness of functional form,[14–16] but simply serves to demonstrate the consistent monotonic behavior of the average ranges with energy. This conclusion lends strong support to our use of Eq. (3) for calculating recoil energies, and the good agreement with predictions of stopping theory (see Appendix) provides further evidence that the Cl^{34m} recoils are produced via a compound-nucleus reaction mechanism over the full range of bombarding energies investigated.

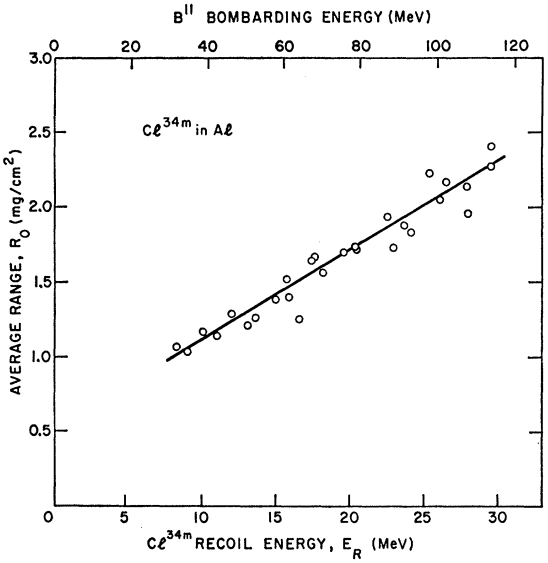

FIG. 4. Range-energy results for the stopping of Cl^{34m} in Al. The solid line is an empirical fit to the data.

B. Angular Distributions

The laboratory angular distribution of Cl^{34m} recoils arises from the effects of nucleon evaporation coupled with the linear momentum transferred from the projectile beam. Consider a compound nucleus with velocity v_c along the beam direction. (v_c is also the velocity of the center-of-mass.) The emission of nucleons gives the residual nucleus a velocity V in the center-of-mass system, directed at a center-of-mass angle θ. In the laboratory system, the recoil nucleus will appear at an angle θ_L given by

$$\theta_L=\tan^{-1}\left(\frac{V\sin\theta}{v_c+V\cos\theta}\right). \quad (5)$$

For all the recoiling nuclei, the laboratory angular distribution will have an average square angle $\langle\theta_L^2\rangle$ given by

$$\langle\theta_L^2\rangle=\tfrac{1}{2}\int_0^\pi\left\{\tan^{-1}\left(\frac{V\sin\theta}{v_c+V\cos\theta}\right)\right\}^2 W(\theta)\sin\theta d\theta, \quad (6)$$

where $W(\theta)$ is the angular distribution of V. It has been shown[2] that for $V\ll v_c$, Eq. (6) becomes

$$\langle\theta_L^2\rangle=c\langle V^2\rangle/v_c^2, \quad (7)$$

with $c=\frac{2}{3}$ for $W(\theta)=1$ and $c=\frac{1}{2}$ for $W(\theta)$ proportional to $1/\sin\theta$. In Eq. (7), the quantity $\langle V^2\rangle$ is the average square of the resultant velocities (in the center of mass) imparted to the recoil nuclei by the emission of particles. (It should be noted that each V, while referring to a single residual nucleus, already contains the contributions from several nucleon emissions, each of which may have its own intrinsic angular distribution.)

Equation (7) relates a characteristic of the laboratory angular distribution to the magnitudes of the center-of-mass velocity and the recoil velocity in the center-of-mass system. The former quantity v_c is considered known in our experiments, and may be obtained from Eq. (3) as

$$v_c^2=2A_bE_b/(A_b+A_T)^2. \quad (8)$$

On the other hand, $\langle V^2\rangle$ is a complex quantity and, while its magnitude is derived from the average total kinetic energy of the emitted particles, there is also a dependence on the energy and angular distributions of these particles. If the compound nucleus emits nucleons isotropically, then $W(\theta)=1$, and under these conditions Simonoff and Alexander[2] have derived the following approximate expression from statistical arguments:

$$\langle V^2\rangle=\frac{8T_n}{(A_T+A_b+A_R)^2}, \quad (9)$$

where T_n is the average total kinetic energy of the emitted nucleons in the center-of-mass system. Combining Eqs. (7), (8), and (9), one obtains, for $W(\theta)=1$,

$$T_n=\frac{3A_b(A_b+A_T+A_R)^2}{8(A_b+A_T)^2}E_b\langle\theta_L^2\rangle. \quad (10)$$

[14] In our experiments, the Cl^{34m} recoil velocities are comparable to those of light fission fragments. It has been shown (see Refs. 15 and 16) for these latter species that range-energy relationships of the forms $R=CE^{1/2}+\Delta$, $R=KE^{2/3}$, and $R=\alpha E^{1/3}+\beta$ are all in agreement with the experimental data.

[15] J. M. Alexander and M. F. Gazdik, Phys. Rev. **120**, 874 (1960).

[16] J. Gilat and J. M. Alexander, Phys. Rev. **136**, B1298 (1964).

TABLE II. Angular distribution results for the $Al^{27}(B^{11},p3n)Cl^{34m}$ reaction.

Bombarding energy, E_b (MeV)	Target thickness, W (mg/cm²)	Angular interval (deg) 0.00	2.37	4.43	6.50	8.53	10.53	12.52	14.48	16.42	18.30	20.15	21.95	23.72	25.42	27.08	Average angle, $\langle\theta_L\rangle$ (deg)	Root-mean-square angle, $\langle\theta_L^2\rangle^{1/2}$ (deg)
		Ring No. 1	2	3	4	5	6	7	8	9	10	11	12	13	14			
		Fractional cross section per unit angle, $\sigma_i/\sigma\Delta\theta_i$ (deg⁻¹)																
59.0	0.38	(0.070)[a]	0.150	0.173	0.179	0.161	0.119	0.071	0.042	0.022	(0.009)	(0.004)					7.86	8.94
58.9	0.93	(0.065)	0.128	0.168	0.168	0.154	0.121	0.086	0.055	0.033	0.016	(0.006)					8.39	9.53
58.6	1.66	(0.069)	0.122	0.145	0.154	0.141	0.117	0.086	0.059	0.041	0.029	0.019	(0.011)	(0.007)			9.04	10.44
76.6	0.49	(0.037)	0.113	0.162	0.172	0.162	0.135	0.097	0.060	0.035	0.018	0.008					8.91	9.94
76.7	0.74	(0.037)	0.124	0.163	0.171	0.159	0.130	0.091	0.061	0.035	0.019	(0.009)					8.83	9.89
76.6	0.81	(0.039)	0.100	0.151	0.173	0.170	0.139	0.093	0.057	0.035	0.022	0.013	(0.008)				9.17	10.27
74.4	1.68	(0.049)	0.106	0.151	0.167	0.161	0.129	0.085	0.055	0.037	0.025	0.017	0.011	(0.007)			9.20	10.44
99.4	0.51	(0.031)	0.103	0.142	0.155	0.151	0.126	0.095	0.068	0.047	0.031	0.020	0.014	(0.010)	(0.007)		9.88	11.18
99.2	0.92	(0.031)	0.103	0.152	0.154	0.149	0.137	0.105	0.059	0.044	0.029	0.018	0.011	0.008			9.64	10.84
98.8	1.66	(0.051)	0.097	0.126	0.146	0.146	0.134	0.104	0.075	0.050	0.032	0.020	0.012	(0.008)			9.79	11.08
114.8	1.66	(0.047)	0.093	0.119	0.140	0.148	0.135	0.106	0.077	0.051	0.034	0.022	0.014	0.009	0.006		10.08	11.42
114.8	1.69	(0.054)	0.096	0.122	0.137	0.138	0.125	0.100	0.077	0.055	0.038	0.024	0.016	0.010	(0.007)		10.08	11.50

[a] Values in parentheses were obtained by graphical extrapolation.

Since $W(\theta)$ refers to the distribution of V, even if there is some anisotropic character in an individual nucleon emission, the smearing over several emissions will result in a diluted effect on $W(\theta)$. In the remainder of this paper we shall assume isotropy of V.[17]

An example of the angular distribution of Cl^{34m} is shown in Fig. 5. Our other experiments are very similar, exhibiting an initial rise, passage through a maximum, and then a relatively gradual decrease in cross section with increasing angle. No significant radioactivity was observed at laboratory angles greater than 27°, even at the highest bombarding energy. The cylindrical geometry of the experiments was such that the radioactivity in a catcher ring is proportional to $d\sigma/d\theta_L$, corresponding to the angular interval subtended by the ring. We have analyzed our data as follows.

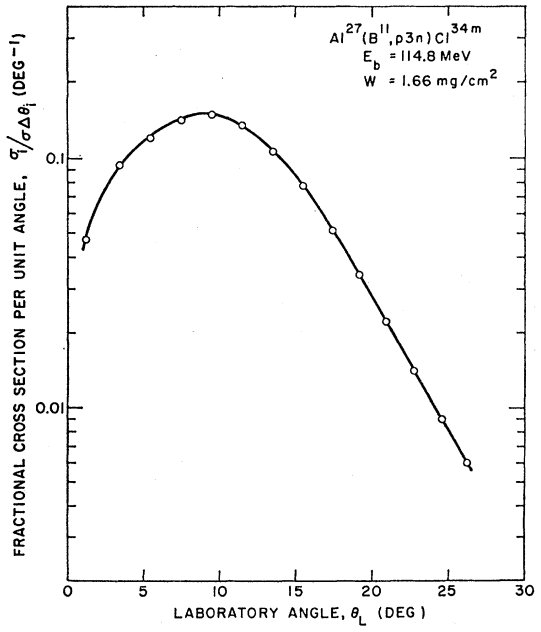

FIG. 5. Typical appearance of a Cl^{34m} angular distribution from the $Al^{27}(B^{11},p3n)$ reaction. This particular case is for a bombarding energy of 114.8 MeV and a target thickness of 1.66 mg/cm².

For each ring, we have evaluated σ_i/σ, where σ_i is proportional to the cross section in the angular interval of ring i, and σ is the total cross section. The quantity σ_i/σ is equivalent to the fractional activity found in ring i. The average square angle $\langle\theta_L^2\rangle$ for the angular distribution was then obtained from

$$\langle\theta_L^2\rangle=\frac{\sum_i[(\sigma_i/\sigma)\langle\theta_i^2\rangle]}{\sum_i(\sigma_i/\sigma)}. \tag{11}$$

The factor $\langle\theta_i^2\rangle$ is the mean-square angle of ring i, taken as

$$\langle\theta_i^2\rangle=(\theta_1^2+\theta_1\theta_2+\theta_2^2)/3, \tag{12}$$

where θ_1 and θ_2 are the defining angles of the ring. The average angle for each angular distribution was calculated using expressions analogous to Eqs. (11) and (12):

$$\langle\theta_L\rangle=\frac{\sum_i[(\sigma_i/\sigma)\langle\theta_i\rangle]}{\sum_i(\sigma_i/\sigma)}, \tag{13}$$

with

$$\langle\theta_i\rangle=(\theta_1+\theta_2)/2. \tag{14}$$

We report our data in Table II. Each angular distribution corresponds to a horizontal row across the table. The first two columns list, respectively, the bombarding energy and target thickness in each experiment. Then we give the fractional cross section per unit angle $(\sigma_i/\sigma\Delta\theta_i)$ for each ring. Also indicated is the angular acceptance of each ring. Finally, the last two columns show the average angle $\langle\theta_L\rangle$, and the root-mean-square angle $\langle\theta_L^2\rangle^{1/2}$ for each experiment.

[17] Even in the extreme case of $W(\theta)$ proportional to $1/\sin\theta$, Eq. (10) does not change in form, but the coefficient $\frac{3}{8}$ becomes $\frac{1}{2}$ (see Ref. 3).

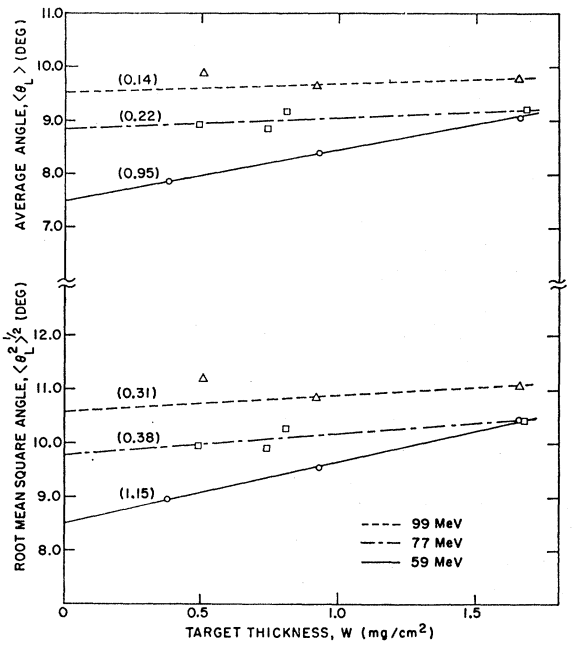

FIG. 6. Experimental dependence of average Cl^{34m} recoil angles on target thickness. The upper set of lines refers to the average laboratory angles $\langle\theta_L\rangle$ and the lower set is for the root-mean-square laboratory angles $\langle\theta_L^2\rangle^{1/2}$. The different lines within each set correspond to the bombarding energies indicated. The numbers in parentheses above each line are the slopes in units of deg/(mg/cm²).

In general, in experiments of this type, systematic errors due to instrumental effects will tend to broaden the angular distributions. This would have its greatest influence at the larger angles because the cross sections are low and these angles are weighted relatively heavily in taking the squares. Consequently, it is of importance to consider such possible effects seriously. The experiments in Table II are in four groups corresponding to four different bombarding energies. At three of these energies we have investigated the effect of target thickness by measuring the angular distributions with several targets. With increasing target thickness, the angular distributions fall off less rapidly at larger angles. We show in Fig. 6 the influence of target thickness on the derived parameters. The top half of the figure is the dependence of the average angle $\langle\theta_L\rangle$ on target thickness, and the lower half refers to the similar dependence of the root-mean-square angle $\langle\theta_L^2\rangle^{1/2}$. The numbers given in parentheses for each line are the empirical slopes in units of deg/(mg/cm²). As can be seen, there is a significant change in slope between the 59-MeV data and the 77-MeV data, but there is not much additional change in going to 99 MeV. In correcting our angular-distribution results for target-thickness effects, we have used the measured dependences at the three energies shown in Fig. 6, and at 114.8 MeV we have assumed that the slope is the same as at 99 MeV. Because of the low cross section for Cl^{34m} at 114.8 MeV, we were unable to make thin-target measurements at this energy.

TABLE III. Average recoil angles and average total energies of particles and photons for the $Al^{27}(B^{11},p3n)Cl^{34m}$ reaction.

Bombarding energy E_b (MeV)	Average angle[a] $\langle\theta_L\rangle$, (deg)	Root-mean square angle[a] $\langle\theta_L^2\rangle^{1/2}$ (deg)	Total available energy, $E_{c.m.}+Q$ (MeV)	Average total particle energy, T_n (MeV)	Average total photon energy, T_γ (MeV)
59.0	7.50	8.50	26.4	19.1	7.3
76.5	8.83	9.79	38.8	32.9	5.9
99.0	9.53	10.56	54.8	49.5	5.3
114.8	9.85	10.94	66.0	61.7	4.3

[a] Corrected for target thickness.

The dependences of average angles on target thickness, as indicated in Fig. 6, are considerably smaller than corresponding data reported for 7–15-MeV Dy recoils.[2] If the observed effects are due primarily to scattering of the recoils in the target material, then the much higher velocities associated with 15–30-MeV Cl^{34m} would imply a smaller target-thickness effect. Also, the larger average angles obtained for Cl^{34m}, as compared to the Dy results, would tend to make this effect less serious. On the other hand, we were unable to measure the target-thickness effects at very small target thicknesses, and if there should be a significant change in slope as zero target thickness is approached, then our values will be in error. We do not believe this is very likely. In support we cite studies of the effects of target thickness on angular distributions of 6–20-MeV Cu^{61} recoils,[18] where measurements with much thinner targets have yielded slopes not very different from our own.

Table III presents the corrected average angles and the de-excitation energies derived from them. The first column lists the bombarding energy, and the second and third columns give, respectively, the average angle $\langle\theta_L\rangle$ and the root-mean-square angle $\langle\theta_L^2\rangle^{1/2}$, each referring to zero target thickness. The fourth column gives the total available energy in the center-of-mass (c.m.) system, which is equivalent to $E_{c.m.}+Q$. This energy is distributed into the c.m. kinetic energies of particle emission and into gamma-ray production. Column 5 is the average total kinetic energy of the emitted nucleons T_n obtained from the data in column 3 by means of Eq. (10). The last column contains the average total energy dissipated as photons, which is simply the difference between columns 4 and 5:

$$T_\gamma=(E_{c.m.}+Q)-T_n. \tag{15}$$

We estimate the uncertainty in $\langle\theta_L^2\rangle^{1/2}$, given in Table III, to be about 0.1°, exclusive of possible systematic errors. This gives rise to an uncertainty of approximately 2% in the derived values of T_n. The effect on the magnitude of T_γ is amplified since the difference

[18] M. Kaplan and V. Subrahmanyam (to be published).

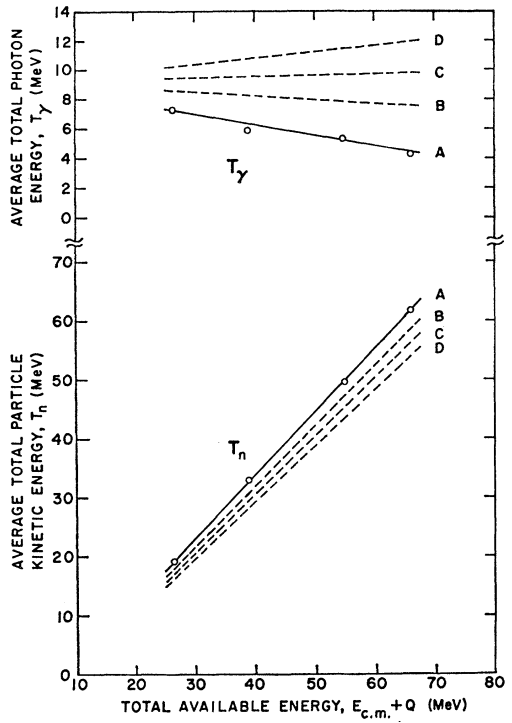

FIG. 7. Average energies of particles and photons, plotted against total available energy in the c.m. system, for the $Al^{27}(B^{11},p3n)Cl^{34m}$ reaction. The lower part of the figure refers to average total kinetic energy of emitted particles T_n and the upper part is for average total gamma-ray energy T_γ. The curves labeled A correspond to our best estimate of the true situation (see text). Curves B, C, and D demonstrate the effects that unrecognized systematic errors would have if they corresponded to 0.3°, 0.5°, and 0.7°, respectively, in the root-mean-square angles. (Note the different scales in the upper and lower parts of the figure.)

between two comparable quantities is involved. As noted previously, systematic errors in our experiments would tend, in general, to make the average angles too large. One such effect may be due to the finite size of the beam collimators. In the work of Simonoff and Alexander[2] on Dy recoils, experimental measurements indicated a correction of 0.3° to $\langle\theta_L^2\rangle^{1/2}$ from this source. However, Croft and Alexander[19] have not found any significant change in the angular distribution of At recoils from $Bi^{209}+He^4$, over a range from $\frac{1}{16}$ in. to $\frac{3}{16}$ in. in collimator size. In our experiments, a reduction in collimator size below the $\frac{1}{8}$-in. level introduced random uncertainties (from poor counting statistics) which were greater than any expected collimator effect. The root-mean-square angles found for Cl^{34m} in our work are comparable to those observed in the experiments of Croft and Alexander,[19] and we assume that no collimator correction is necessary.

It is useful, nevertheless, to consider what influence systematic errors may have on the interpretation of our results. We have plotted in Fig. 7 the values of T_n (lower curves) and T_γ (upper curves) versus total available energy $E_{c.m.}+Q$. The lines designated A correspond to the data in Table III, and represent our best estimate of the true situation. Curves B, C, and D indicate the changes which occur when "corrections" of 0.3°, 0.5°, and 0.7°, respectively, are subtracted from the root-mean-square angles. As can be seen from Fig. 7, the qualitative behavior of T_n does not change very much, and the more sensitive T_γ values do not begin to reverse their trend with energy until unreasonably large systematic errors are assumed.

Hence, we conclude from our angular-distribution studies, that in the production of Cl^{34m}, the compound nucleus dissipates most of its energy as kinetic energies of the emitted particles. The increase in total particle kinetic energy is linear with total available energy over the energy region investigated. The total energy which is released in the form of gamma radiation is relatively small, certainly less than 10 MeV, and seems to show a decrease with increasing available energy. These results imply that there is no appreciable gamma-ray competition with particle emission in the processes leading to Cl^{34m}.

The conclusions of the above paragraph appear, to us at least, somewhat surprising. If significant gamma-ray emission in compound-nucleus de-excitation is indeed an indicator of high angular momentum,[20] then apparently Cl^{34m} (with nuclear spin-3 compared to a spin-0 ground state) does not arise by a preferential selection from nuclear interactions of high angular momentum. An alternative explanation is that the angular momentum is removed largely by the emitted particles. If this were the case, the particles would exhibit enhanced forward-backward peaking, a similar effect would be present in the angular distribution of V, and our data would require that even more of the total available energy be consumed as particle kinetic energies (with essentially no gamma-ray energy remaining).

Previous studies of the de-excitation of Dy compound nuclei[2,3] have indicated that there is significant gamma-ray competition with neutron emission leading to Dy products. Furthermore, the energy dissipated as gamma radiation increases rapidly with available energy. In the same work, de-excitation of Tb compound nuclei to the low-spin isomer Tb^{149g} was found to be associated with forward-backward peaking of the emitted neutrons and very little gamma-ray production. Our results for Cl^{34m} do not fit in with this picture. Hence, it may be that the details of compound-nucleus de-excitation processes are not general but are strongly related to the mass region one is investigating. A likely origin of such a mass dependence could be in the character of the nuclear level densities at high excitation. It is worth pointing out that in the $Al^{27}+B^{11}$ reaction at the energies considered here, the internal excitation gets as high as 2 MeV per particle of the compound system. In the heavier mass region,

[19] P. D. Croft and J. M. Alexander (unpublished data).

[20] J. R. Grover, Phys. Rev. **127**, 2142 (1962).

comparable total excitation energies correspond to substantially less than 1 MeV per particle.

In discussing the behavior of the $Al^{27}(B^{11},p3n)Cl^{34m}$ excitation function in Sec. IIIA, above, we noted the rather slow decrease in cross section at energies above the excitation function peak. If gamma-ray emission were competitive with nucleon evaporation at the higher energies, then one could argue that the production of photons drained sufficient energy from the system to leave the residual nuclei in states of excitation too low to emit an additional particle. However, as our results indicate otherwise, it is not at all clear why the excitation function does not decrease more rapidly with energy.

Perhaps, at the very high excitation energies (per particle) encountered here, the concept of a compound-nucleus reaction within the usual statistical model framework[21,22] begins to lose some of its validity. As bombarding energies increase, one would expect a decrease in the fraction of the total reaction cross section which goes into compound-nucleus processes. In addition, it is likely that those interactions which occur at large classical impact parameters would be lost sooner than would "head-on" collisions. These qualitative arguments are consistent with our observations of relatively low Cl^{34m} cross sections and little evidence of high angular momentum. Furthermore, even those processes which remain in the compound-nucleus category may, at some energy, be so highly excited that the onset of particle emission occurs before statistical thermal equilibrium has been fully attained. Under such conditions, it would no longer be appropriate to consider the excited nucleus as possessing a unique nuclear temperature, since the temperature corresponding to the energies of the emitted particles may be considerably higher than the average temperature. Related questions of compound-nucleus lifetimes at very high excitation would also have to be considered. Admittedly, we are indulging in speculation, but if these ideas have some applicability to our experimental circumstances, then the observed kinetic energies of emitted particles have a "natural" explanation. It would then be the high particle energies which lead to the excitation-function behavior, rather than the converse.

IV. SUMMARY

Our recoil-range and angular-distribution studies of the $Al^{27}(B^{11},p3n)Cl^{34m}$ reaction have led us to the following conclusions. (a) The reaction proceeds by compound-nucleus formation over the full-energy region investigated, $E_b=30$ to 115 MeV. (b) Most of the available de-excitation energy is dissipated as kinetic energy of the emitted particles. (c) The total kinetic energy of emitted particles increases approximately linearly with available energy. (d) The amount of energy released in the form of gamma radiation is relatively small, of the order of 7 MeV or less. (e) The trend of gamma-ray emission energy with increasing available energy is roughly constant, but seems to show a slight decrease. (f) The above results for the high-spin isomer Cl^{34m} do not fit in with expectations based upon previous studies of the de-excitation of Dy and Tb compound nuclei. (g) No straightforward explanation has been found for the excitation function behavior (relatively slow falloff) at higher energies, unless the very high excitation energies (per particle) involved lead to a rapid onset of particle emission from a nonequilibrium compound system.

ACKNOWLEDGMENTS

We would like to thank the operating staff of the Yale HILAC for their extra efforts in getting beam through our collimators, and Mrs. Peggy Ewart for her assistance in several phases of the experimentation. Our appreciation is extended to Professor John M. Alexander, Dr. Paul Croft, and Dr. Joe Natowitz for many useful discussions and for making available some of their unpublished data. We thank Professor Richard Wolfgang and Professor Alexander for critically reading the manuscript and their helpful comments thereon. Finally, we acknowledge the excellent performance of Mrs. Margaret Gural in the typing of several drafts of this paper.

APPENDIX

The range-energy data for Cl^{34m} in Al obtained in this work provide a useful test of the theoretical relationships developed by Lindhard, Scharff, and Schiott (LSS).[23] We shall first briefly outline the LSS theory and then compare our results with its predictions.

LSS consider the stopping of energetic heavy ions in matter as arising from electronic collisions (ionization) and nuclear collisions (ion-atom interaction), with the two processes being taken as uncorrelated and continuous. A Thomas-Fermi (statistical) model is used as a basis for the ion-atom interaction, and electronic stopping is assumed to be proportional to velocity. For an ion of mass M_R and nuclear charge Z_R, moving in a stopping medium of atomic mass M_S and nuclear charge Z_S, the kinetic energy E_R and corresponding true range R (total path length) are expressed as dimensionless (reduced) variables ϵ and ρ_L given by

$$\epsilon=\frac{E_R a M_S}{Z_R Z_S e^2(M_R+M_S)}, \tag{A1}$$

$$\rho_L=RNM_S(4\pi)a^2\frac{M_R}{(M_R+M_S)^2}, \tag{A2}$$

where

$$a=0.8853(\hbar^2/me^2)(Z_R^{2/3}+Z_S^{2/3})^{-1/2} \tag{A3}$$

[21] T. Ericson, Phil. Mag. Suppl. **9**, 425 (1960).
[22] D. Bodansky, Ann. Rev. Nucl. Sci. **12**, 79 (1962).
[23] J. Lindhard, M. Scharff, and H. E. Schiott, Kgl. Danske Videnskab. Selskab, Mat. Fys. Medd. **33**, No. 14 (1963).

is a Thomas-Fermi screening length, m and e are the mass and charge of an electron, N is the atomic density of the stopping medium, and $\hbar$ is Planck's constant divided by 2π. In the approximation that the energy loss in nuclear and electronic stopping are independent, the total stopping power is expressed as a linear combination of the two contributions:

$$\left(\frac{d\epsilon}{d\rho_L}\right)=\left(\frac{d\epsilon}{d\rho_L}\right)_n+\left(\frac{d\epsilon}{d\rho_L}\right)_e. \quad \text{(A4)}$$

Assuming electronic stopping to be proportional to velocity,

$$(d\epsilon/d\rho_L)_e=k\epsilon^{1/2} \quad \text{(A5)}$$

LSS obtain from Eqs. (A4) and (A5) a range-energy relationship:

$$\rho_L(\epsilon)=\tfrac{1}{2}k\epsilon^{1/2}-\Delta(k,\epsilon), \quad \text{(A6)}$$

where $\Delta(k,\epsilon)$ represents the effect of nuclear stopping and is treated as a correction to the electronic range. The parameter k characterizes the static properties of the moving ion and the stopping medium. An approximate expression for this parameter is given as

$$k=\xi\left[\frac{0.0793Z_R^{1/2}Z_S^{1/2}(M_R+M_S)^{3/2}}{(Z_R^{2/3}+Z_S^{2/3})^{3/4}M_R^{3/2}M_S^{1/2}}\right];\quad \xi\approx Z_R^{1/6}. \quad \text{(A7)}$$

The theoretical estimates of $\Delta(k,\epsilon)$ as a function of ϵ are presented by LSS for various values of k.

In our experiments, the observed Cl^{34m} recoil energies correspond to rather high velocities. Translated into the LSS scheme via Eq. (A1), our data cover the region $\epsilon=150$ to $\epsilon=550$. One would expect, from the theoretical formulation, the predominant energy-loss process to be electronic stopping, and hence the theoretical predictions are relatively insensitive to the contribution from nuclear stopping. This implies that a comparison of our results with the calculated ranges is primarily testing the assumption of proportionality of electronic stopping to velocity, and the description of the parameter k.

Figure 8 is a ρ_L versus ϵ representation of our range-energy results from Table I. The solid curves are the range-energy relationships calculated from the LSS theory for several values of k. These curves have been corrected from true to projected ranges, in the manner prescribed by LSS, and are directly comparable to the experimental data. The general concurrence between theory and experiment is quite good, both in the magnitudes of the ranges and in their trend with energy. The extent of quantitative agreement is very likely within the accuracy sought by the theory. Closer inspection, however, reveals several features which may indicate a direction for further exploration. First, the experimental points fall systematically below the curve for $k=0.13$, which Eq. (A7) gives as the theoretical parameter for Cl^{34} in Al. Second, the variation of the observed ranges with energy does not follow very closely the theoretical curvature resulting from a velocity dependence of electronic stopping. The experimental points seem to correspond to a somewhat higher power dependence, more nearly that of energy.

The LSS theory takes no account of the details of atomic structure, and it is possible that the deviations discussed here are due to the particular chemistry of Cl. Further experiments in the electronic stopping region should determine the generality or specificity of this behavior.

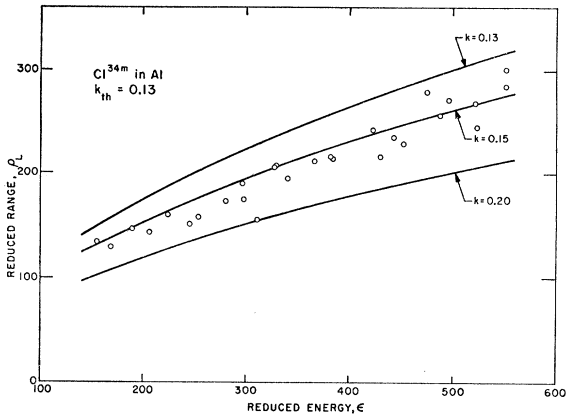

FIG. 8. Reduced range ρ_L versus reduced energy ϵ for Cl^{34m} stopping in Al. The points are the experimental results from Table I. The solid curves are theoretical predictions, based on Ref. 23, for several values of the electronic stopping parameter k.